El-Maiss, J., Darmanin, T., Taffin De Givenchy, E., Amigoni, S., Eastoe, J., Sagisaka, M., & Guittard, F. (2014). Superhydrophobic surfaces with low and high adhesion made from mixed (hydrocarbon and fluorocarbon) 3,4-propylenedioxythiophene monomers. *Journal of Polymer Science Part B - Polymer Physics*, *52*(11), 782-788. https://doi.org/10.1002/polb.23483

Superhydrophobic Surfaces with Low and High Adhesion Made from Mixed (Hydrocarbon and Fluorocarbon) 3,4-Propylenedioxythiophene Monomers

Janwa El-Maiss,[1] Thierry Darmanin,[1] Elisabeth Taffin de Givenchy,[1] Sonia Amigoni,[1] Julian Eastoe,[2] Masanobu Sagisaka,[3] Frédéric Guittard[1]*

1: Univ. Nice Sophia Antipolis, CNRS, LPMC, UMR 7336, Nice 06100, France
2: School of Chemistry, University of Bristol, Bristol, BS8 1TS, UK
3: Department of Frontier Materials Chemistry, Graduate School of Science and Technology, Hirosaki University, Japan
Correspondence to: Frédéric Guittard (E-mail: *guittard@unice.fr*)

ABSTRACT

This work concerns new superhydrophobic surfaces, generated by replacing long fluorocarbon chains, which bioaccumulate, with short chains whilst at the same time retaining oleophobic properties. Here, is described the synthesis of novel 3,4-propylenedioxythiophene derivatives containing both a short fluorocarbon chain (perfluorobutyl) and a hydrocarbon chain of various lengths (ethyl, butyl and hexyl). Superhydrophobic (θ_{water} > 150°) surfaces with good oleophobic properties (60° > $\theta_{hexadecane}$ > 80°) have been obtained by electrodeposition using cyclic voltammetry. Surprisingly, the lowest hystereses and sliding angles (Lotus effect) are obtained with the shortest alkyl chains due to the presence of microstructures made of nanofibers on the surfaces, whereas, the longest alkyl chains leads to nanosheets with high adhesion (Petal effect). Such materials are potential candidates for biomedical applications.

KEYWORDS: Superhydrophobic Surfaces, Electrochemistry, Conducting polymers, Wettability

INTRODUCTION

Superhydrophobic surfaces are highly in demand for their various potential applications in self-cleaning windows,[1] anticorrosion,[2] anti-icing,[3] antibacterial,[4] cell/protein adhesion,[5] smart materials,[6] oil/water separation membranes,[7] for example. Such performance can be obtained combining low surface energy materials with the formation of surface structures, as observed on natural surfaces.[8-9] For fluorocarbon, hydrocarbon and silicone materials used as low surface energy materials, several strategies can be used to form surface structures.[8-9]

The formation of surface structures can also, for example, be performed by electrodeposition of conducting polymers.[9-15] This process corresponds to the oxidation of monomers present in solution using an electrochemical system to deposit the corresponding conducting polymer film on the working electrode. If the monomers are substituted with hydrophobic substituents, that can result in a one-pot process.[16-20] The formation of surface structures and the surface hydrophobicity/oleophobicity depend implicitly on electrochemical parameters but also on the monomer structures. The nature of the monomer is highly important and 3,4-propylenedioxythiophene (ProDOT) is an ideal template for several reasons including its exceptional polymerization capacity and the possibility to introduce substitution several positions.[16-24] Moreover, the surface morphology of poly(3,4-propylenedioxythiophene) (PProDOT) importantly depends on intrinsic hydrophobicity of the substituents and various morphologies going from nanofibers

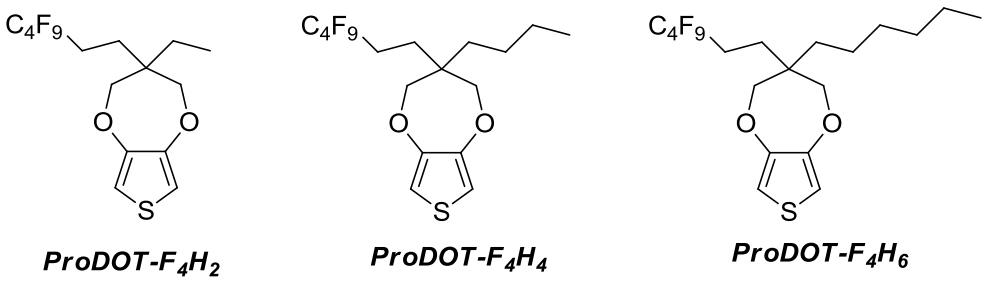

SCHEME 1 Mixed original monomers synthesized in this manuscript.

(for highly hydrophilic substituents) to cauliflower-like structures (for highly hydrophobic substituents) as has been.[21-24] Usually, fluorocarbon and hydrocarbon chains are used to increase the surface hydrophobicity but only fluorocarbon chains can be used to generate surface oleophobicity. However, chemicals with long fluorocarbon chains are known to bioaccumulate in animals and humans.[25-26]

To overcome the problems associated with long fluorocarbon chains in the generation of superhydrophobic surfaces, different strategies have been developed: the use of hydrocarbon derivatives as found in Nature, often leading also to superoleophilic properties, and/or the use of short fluorocarbon chains (perfluorobutyl or C_4F_9, for example). Indeed, it has been demonstrated that the bioaccumulative potential of fluorocarbons depends on chain length, and that those with seven or less perfluoromethylene units can be considered as non-bioaccumulative.[25-26]

Here, we report for the first time the study of the surface morphology and wettability of electrodeposited mixed (hydrocarbon and fluorocarbon) conducting polymers. The three original monomers derived from ProDOT and represented in Scheme 1 were synthesized by substitution of ProDOT in the 3-position by both a hydrocarbon chain and a fluorocarbon chain. The corresponding polymers were characterized by scanning electron microscopy (SEM) and by measurements of apparent and dynamic contact angles using different probe liquids (water, diiodomethane, hexadecane) to determine the surface hydrophobicity and oleophobicity.

EXPERIMENTAL

The general procedure to synthesize the monomers is represented in Scheme 2. All chemicals were purchased from Sigma Aldrich. Diethyl 2-(3,3,4,4,5,5,6,6,6-nonafluorohexyl)malonate (**1**) was synthesized using a procedure reported in the literature.[27-29] The synthesis of the other intermediates (**2a**, **2b**, **2c**, **3a**, **3b**, **3c** as represented in Scheme 2) is described below.

Monomer synthesis and characterization

Synthesis of diethyl 2-ethyl-2-(3,3,4,4,5,5,6,6,6-nonafluorohexyl)malonate (2a)

Sodium hydride (2 eq., 20 mmol) was dissolved in 100mL anhydrous tetrahydrofuran (THF). Then 1 (1 eq., 10 mmol) was added drop-wise. After stirring for 30 min, diethyl sulfate (1 eq., 10mmol) was added and the mixture was heated under reflux for 48 hr. The solvent was evaporated under reduced pressure, then 40 mL of water was added, and the organic mixture was extracted by diethyl ether. The collected organic phases were washed using brine, dried over anhydrous Na_2SO_4.

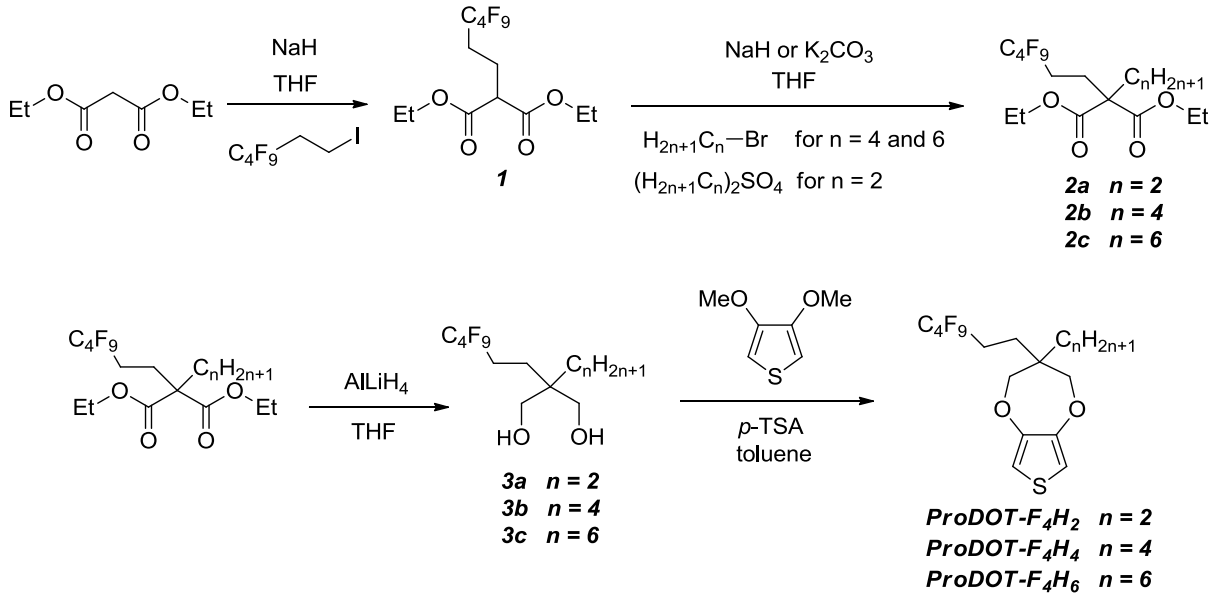

SCHEME 2 Synthesis route to the monomers.

Purification was done by flash chromatography on silica gel (7:3 chloroform:cyclohexane) to obtain the pure product.
Yield 25%; Colourless liquid; ^{1}H NMR (200 MHz, $CDCl_3$, δ): 4.21 (q, *J* = 7.1 Hz, 4H), 2.14 (m, 4H), 1.95 (q, 2H, *J* = 7.1 Hz), 1.25 (t, 6H, *J* = 7.1 Hz), 0.86 (t, 3H, *J* = 7.1 Hz).

Synthesis of diethyl 2-butyl-2-(3,3,4,4,5,5,6,6,6-nonafluorohexyl)malonate (2b) and diethyl 2-hexyl-2-(3,3,4,4,5,5,6,6,6-nonafluorohexyl)malonate (2c)

2b and 2c were synthetized as described in the literature[27-29] mixing K_2CO_3 (1.2 eq., 26 mmol) of tetrabutylammonium bromide (TBAB) (0.5 eq., 11 mmol), **1** (1 eq., 22 mmol) and the corresponding 1-bromoalkane (1 eq., 22 mmol) in 100 mL of THF. The mixture was heated under reflux for 48 hr. After cooling to room temperature, salts were filtrated and washed with ethyl acetate. The solvent was evaporated, and the mixture was distilled under pressure to obtain the products.

Diethyl 2-butyl-2-(3,3,4,4,5,5,6,6,6-nonafluorohexyl)malonate (2b): Yield 45%; Colourless liquid; ^{1}H NMR (200 MHz, $CDCl_3$, δ):4.16 (q, 4H, *J* = 7.2 Hz), 2.10 (m, 4H), 1.84 (m, 2H), 1.20 (m, 10H), 0.85 (t, 3H, *J* = 6.6 Hz).
Diethyl 2-hexyl-2-(3,3,4,4,5,5,6,6,6-nonafluorohexyl)malonate (2c): Yield 76%; Colourless liquid; ^{1}H NMR (200 MHz, $CDCl_3$, δ): 4.20 (q, 4H, *J* = 7.2 Hz), 2.15 (m, 4H), 1.87 (m, 2H), 1.23 (m, 14H), 0.87 (t, 3H, *J* = 6.6 Hz).

Synthesis of 2-alkyl-2-(3,3,4,4,5,5,6,6,6-nonafluorohexyl)propane-1,3 diol

Compound **2** (1 eq., 5 mmol) was added to a solution of $LiAlH_4$ (2.5 eq., 12 mmol) in 100 mL of diethyl ether in an ice bath. The reaction mixture was stirred at 40 °C overnight. A mixture of ammonium chloride and diethyl ether was added, and then HCl (1N) was added to neutralize the remaining aluminum salts. The aqueous mixture was extracted with diethyl ether. The collected organic phases were

washed using brine, dried over anhydrous Na_2SO_4, affording to the diol.

2-ethyl-2-(3,3,4,4,5,5,6,6,6-nonafluorohexyl)propane-1,3 diol (3a): Yield 90%; Colourless liquid; ^{1}H NMR (200 MHz, $CDCl_3$, δ): 3.64 (d, 2H, *J* = 10.6 Hz), 3.53 (d, 2H, *J* = 10.6 Hz), 2.10 (m, 2H), 1.66 (m, 2H), 1.27 (m, 2H), 0.84 (t, 3H, *J* = 7.5 Hz).

2-butyl-2-(3,3,4,4,5,5,6,6,6-nonafluorohexyl)propane-1,3 diol (3b): Yield 93%; Colourless liquid; ^{1}H NMR (200 MHz, $CDCl_3$, δ): 3.62 (d, 2H, *J* = 10.6 Hz), 3.51 (d, 2H, *J* = 10.6 Hz), 2.08 (m, 2H), 1.69 (m, 2H), 1.20 (m, 6H), 0.90 (t, 3H, *J* = 7.5 Hz).

2-hexyl-2-(3,3,4,4,5,5,6,6,6-nonafluorohexyl)propane-1,3 diol (3c): Yield 92%; Colourless liquid; ^{1}H NMR (200 MHz, $CDCl_3$, δ): 3.65 (d, 2H, *J* = 10.6 Hz), 3.54 (d, 2H, *J* = 10.6 Hz), 2.07 (m, 2H), 1.67 (m, 2H), 1.22 (m, 10H), 0.88 (t, 3H, *J* = 7.5 Hz).

Synthesis of ProDOT-F$_4$H$_n$

3,4-dimethoxythiophene (1 eq., 2.6 mmol), the corresponding diol (1 eq., 2.6 mmol) and p-toluenesulfonic acid (0.3 mmol) were added to 30 mL of toluene. After stirring for two days at 90°C, the product was purified by column chromatography gel (eluent; 1:1 dichloromethane:cyclohexane).

3-ethyl-3-(3,3,4,4,5,5,6,6,6-nonafluorohexyl)-3,4-dihydro-2*H*-thieno[3,4-*b*][1,4]dioxepine (ProDOT-F$_4$H$_2$): Yield 42%; Colourless liquid; ^{1}H NMR (200 MHz, $CDCl_3$, δ): 6.46 (2H, s), 3.91 (d, 2H, *J* = 12.2 Hz), 3.83 (d, 2H, *J* = 12.2 Hz), 2.11 (m, 2H), 1.76 (m, 2H), 1.42 (q, 2H, *J* = 7.5 Hz), 0.90 (t, 3H, *J* = 7.5 Hz); ^{19}F NMR (188 MHz, $CDCl_3$, δ): -81.05, -115.20, -124.17, 126.08; ^{13}C NMR (200 MHz, $CDCl_3$, δ): 149.29, 105.16, 76.40, 43.05, 25.04 (t, *J* = 22.5 Hz), 24.55, 24.77, 21.31 (t, *J* = 3.8 Hz), 7.08; IR (KBr): *v* = 3118, 2971, 2885, 1488, 1377, 1233, 1133 cm^{-1}; EIMS (*m/z* (%)): 430 (40) [M^+], 141 (7) [$C_6H_5O_2S^+$], 127 (18) [$C_4H_7OS^+$], 116 (100) [$C_4H_4O_2S^+$].

3-butyl-3-(3,3,4,4,5,5,6,6,6-nonafluorohexyl)-3,4-dihydro-2*H*-thieno[3,4-*b*][1,4]dioxepine (ProDOT-F$_4$H$_4$): Yield 37%; Colourless liquid; ^{1}H NMR (200 MHz, $CDCl_3$, δ): 6.46 (s, 2H), 3.91 (d, 2H, *J* = 12.3 Hz), 3.83 (d, 2H, *J* = 12.3 Hz), 2.11 (m, 2H), 1.77 (m, 2H), 1.31 (m, 6H), 0.92 (t, 3H, *J* = 6.8 Hz); ^{19}F NMR (188 MHz, $CDCl_3$, δ): -81.05, -115.18, -124.17, 126.08; ^{13}C NMR (200 MHz, $CDCl_3$, δ): 149.29, 105.15, 76.68, 43.04, 32.00, 25.12 (t, *J* = 21.4 Hz), 24.77, 21.96 (t, *J* = 3.5 Hz), 13.88; IR (KBr): *v* = 3118, 2959, 2870, 1488, 1379, 1231, 1133 cm^{-1}; EIMS (*m/z* (%)): 458 (40) [M^+], 40), 141 (15) [$C_6H_5O_2S^+$], 127 (18) [$C_4H_7OS^+$], 116 (100) [$C_4H_4O_2S^+$].

3-hexyl-3-(3,3,4,4,5,5,6,6,6-nonafluorohexyl)-3,4-dihydro-2*H*-thieno[3,4-*b*][1,4]dioxepine (ProDOT-F$_4$H$_6$): Yield 38%; Colourless liquid; ^{1}H NMR (200 MHz, $CDCl_3$, δ): 6.46 (s, 2H), 3.91 (d, 2H, *J* = 12.2 Hz), 3.83 (d, 2H, *J* = 12.2 Hz), 2.11 (m, 2H), 1.77 (m, 2H), 1.28 (m, 10H), 0.88 (t, 3H, *J* = 5.9 Hz); ^{19}F NMR (188 MHz, $CDCl_3$, δ): -81.03, -115.13, -124.15, 126.04; ^{13}C NMR (200 MHz, $CDCl_3$, δ): 149.29, 105.14, 76.68, 43.08, 32.29, 31.57, 29.96, 25.12 (t, *J* = 22.5 Hz), 22.54, 21.95 (t, *J* = 3.7 Hz), 13.97; IR (KBr): *v* = 3114, 2959, 2862, 1488, 1379, 1237, 1133 cm^{-1}; EIMS (*m/z* (%)): 486 (45) [M^+], 141 (6) [$C_6H_5O_2S^+$], 127 (11) [$C_4H_7OS^+$], 116 (100) [$C_4H_4O_2S^+$].

Electrochemical deposition

The depositions were performed using an Autolab potentiostat of Metrohm. Electrode plates, consisting in a deposition of 20 nm chromium and 150 nm gold on silicon wafer were purchased from Neyco. Glassy carbon rods were purchased from Metrohm. Saturated calomel electrodes (SCE) were purchased from Radiometer analytical. For the experiments, a glass cell was connected to the potentiostat *via* a three-electrode system: a gold plate as working electrode, a carbon rod as counter-electrode and a SCE as reference electrode. 10 mL of anhydrous acetonitrile containing 0.1 M of tetrabutylammonium perchlorate (Bu_4NClO_4) was put inside the glass cell.

TABLE 1 Contact angles of water, diiodomethane and hexadecane of the polymer surfaces.

Polymer	Number of scans	θ_{water}	H_{water}	α_{water}	θ_{diiodo}	$\theta_{hexadecane}$
PProDOT-F_4H_2	1	156.1	Sticking behaviour		105.5	62.3
	3	160.3	3.3	2.0	136.0	69.7
	5	160.4	0.4	0.6	145.8	61.3
PProDOT-F_4H_4	1	141.3	Sticking behaviour		112.3	76.3
	3	142.7	Sticking behaviour		111.6	74.2
	5	159.0	7.9	5.1	124.7	70.7
PProDOT-F_4H_6	1	132.2	Sticking behaviour		100.0	67.4
	3	139.0	Sticking behaviour		112.8	61.9
	5	153.2	Sticking behaviour		111.7	67.5

After degassing under argon, the monomer oxidation potential was determined by cyclic voltammetry ($E^{ox} \approx 1.60$ V *vs* SCE). Then, the depositions were also performed by cyclic voltammetry (between -1 V *vs* SCE and a potential slightly lower to E^{ox}) which allows these monomers to polymerize on the surfaces as highly adherent and homogeneous films. Here, the films were deposited with a scan rate of 20 mV s^{-1} and after one, three and five scans. An example cyclic voltammogram is given in Figure 1. Steric hindrance, due to the sizes of the two substituents was observed for each monomer (the polymer oxidation potential increases as the increase in the number of scans). Finally, the substrates were washed with acetonitrile and dried in a vacuum oven over night.

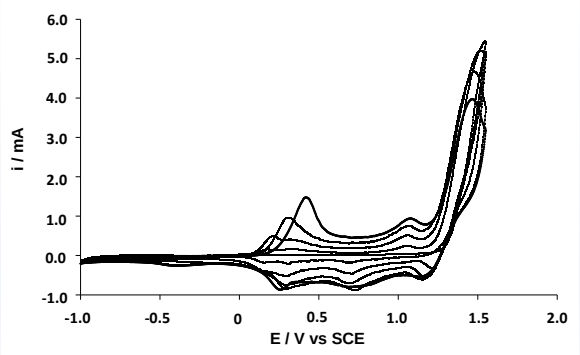

FIGURE 1 Cyclic voltammogram of ProDOT-F_4H_2 (0.01 M) in anhydrous acetonitrile containing 0.1 M of Bu_4NClO_4; Scan rate: 20 mV s^{-1}.

Surface analyses

The surface wettability was determined by apparent and dynamic contact angle measurements using a DSA30 goniometer (Krüss). Three liquids of different surface tensions were used: water (γ_L = 72.8 mN/m), diiodomethane (γ_L = 50.0 mN/m) and hexadecane (γ_L = 27.6 mN/m). The apparent contact angles were obtained with the sessile drop method and the dynamic contact angles with the tilted-drop method. After surface inclination, the hysteresis ($H = \theta_{adv} - \theta_{rec}$) was determined just before the droplet rolled off the surface. The maximum surface inclination is called sliding angle (α). The surface structures were observed by SEM images with a 6700F microscope of JEOL.

RESULTS AND DISCUSSION

Surface wettability

The apparent and dynamic contact angle measurements of the polymer films electrodeposited by cyclic voltammetry are gathered in Table 1 and Figure 2. The highest repellency surfaces were obtained after five scans.

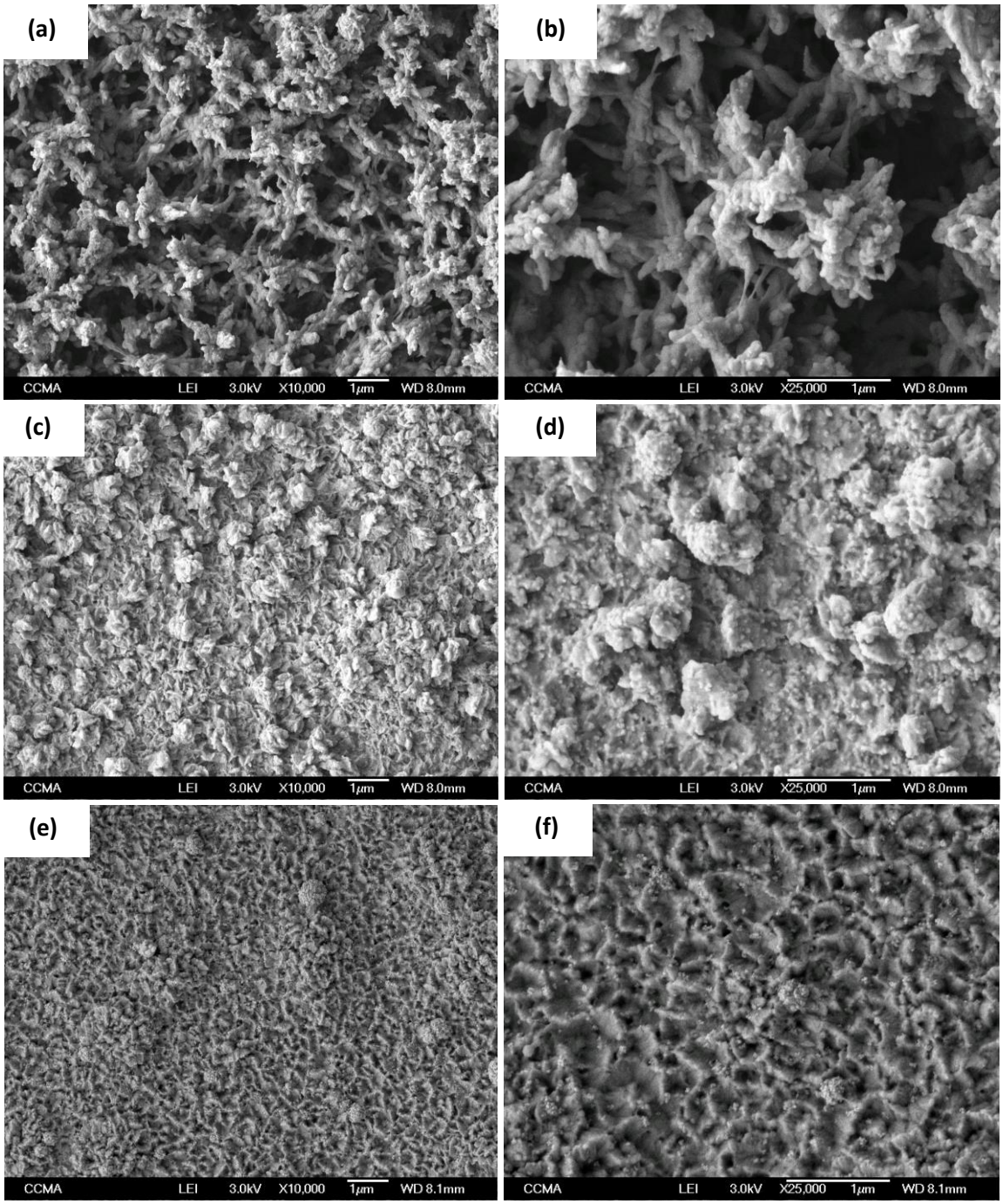

FIGURE 3 SEM images of (a,b) PProDOT-F_4H_2, (c,d) PProDOT-F_4H_4 and (e,f) PProDOT-F_4H_6 for two different magnifications (x 10000 and x 25000); Number of scans: 5.

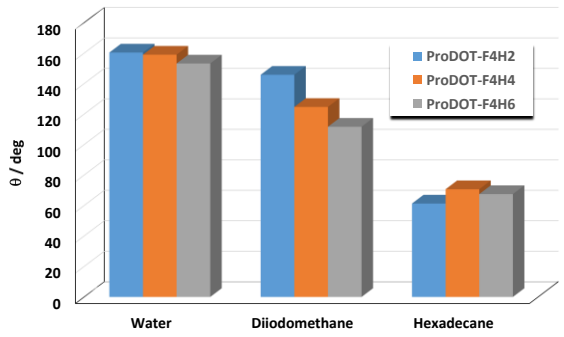

FIGURE 2 Apparent contact angles of water, diiodomethane and hexadecane for the polymers; Number of scans: 5.

Surprisingly, superhydrophobic surfaces were obtained with the three polymers but extremely low hysteresis (H) and sliding angles (α) were recorded only for the films made using the shortest alkyl chain length (H = 0.4 and α = 0.6 for PProDOT-F_4H_2 and H = 7.9 and α = 5.1 for PProDOT-F_4H_4).

By contrast, water droplets deposited on PProDOT-F_4H_6 remained stuck showing extremely high adhesion. PProDOT-F_4H_2 showed also the highest repellency properties for diiodomethane. However, the influence of the alkyl chain length on the apparent contact angle of hexadecane was not significant and did not exceed 80°.

Surface structures

To explain the differences observed in wettability, the surface morphologies were investigated by SEM, and images of the polymer-coated surfaces are given in Figure 3. The most structured surfaces were obtained for PProDOT-F_4H_2. This surface was composed of microstructures made of nanofibers, explaining the extremely high repellent properties measured on this surface. Indeed, it was demonstrated in the literature that the presence of nanofibers on a surface can lead to extremely high apparent water contact angles with extremely low H and α.[30] Here, the increase in the alkyl chain length induced a notable change in surface morphology from nanofibers to nanosheets, accompanied by an decrease in surface roughness. This change in surface morphology can be explained by the decrease in the solubility of the oligomers formed in the initial stages of electropolymerization in agreement with literature.[31] Indeed, in a very polar solvent (acetonitrile), it is expected that the polymer solubility decreases with increasing alkyl chain length.

Discussion

The differences observed in the surface wettability of the three polymers can be explained using the Wenzel ($\cos\theta = r\cos\theta^Y$ with r a roughness parameter and θ^Y Young's angle) and Cassie-Baxter ($\cos\theta = f\cos\theta^Y + f - 1$ with f the solid fraction and (1 - f) the air fraction) equations.[32-33] Because these two equations depend on θ^Y,[34] we have first prepared a "smooth" surface for each polymer. The smooth surfaces were obtained changing the deposition method (deposition at constant potential) and using an extremely short deposition charge (Qs = 1 mC cm^{-2}). Indeed, in the initial stages of electropolymerization only a smooth layer of polymer covering all of the working electrode was obtained, and the formation of nanostructures only occurs a little after this period. The values of θ^Y are gathered in Table 2. The polymers are intrinsically hydrophobic ($\theta^Y_{water} > 90°$) and intrinsically oleophilic ($\theta^Y_{hexadecane} < 90°$). As expected, the contact angle for water increased with alkyl chain length because it depends on the number of CF_3 and CH_3 groups present at the outer surface. A decrease was observed for the contact angles with hexadecane because they should increase with the CF_3 groups but decrease with the number of CH_3 groups (two opposite effects). Now, the Wenzel and Cassie-Baxter equations will be used to explain the different wettabilities of the polymer films. When a liquid

droplet is in the Wenzel state,[32] the droplet fully wets the rough surface leading to an increase in the solid-liquid interface due to the roughness. Here, the roughness increases the surface hydrophobicity/oleophobicity of intrinsically hydrophobic/oleophobic materials, and reversely. Moreover, due to the increase in the solid-liquid interface area, there is an increase in the roughness which leads increases in H and α. By contrast, when a liquid droplet is in the Cassie-Baxter state,[33] it is suspended on top of the surface roughness and on air present between the droplet and the surface. This time, the increase in liquid-vapor interface area due to the presence of air increases the apparent contact angle but decreases H and α. This behavior is more often called the "Lotus Effect" and is associated with the self-cleaning properties of lotus leaves. The ultra-low adhesion and hysteresis of water droplets during rainfall allows the leaf surfaces to be both clean and dry.[8,9,35] Moreover, it was demonstrated that structure formation at both the micro and nanoscale is a way to produce highly robust superhydrophobic properties.[36-39] Intermediate states (between the Wenzel and Cassie-Baxter state) can also exist. For example, a Cassie-Baxter impregnating state was observed on the surface of red rose petal (Petal effect).[40] Indeed, when a water droplet is deposited on this surface, it remains stuck even after inclination of 180°, indicating of extremely high adhesion. This is due to the fact that water droplets enter into the large grooves of the petal but not into the small ones. In the cases described here, for a scan number = 5, water droplets deposited on PProDOT-F_4H_2 and PProDOT-F_4H_4 surfaces were in the Cassie-Baxter state (Lotus effect) thanks to the presence of micro- and nanostructures, whereas, water droplets deposited on PProDOT-F_4H_6 were in a Cassie-Baxter impregnating state (Petal effect) owing to the presence of nanosheets. Moreover, the polymers are intrinsically oleophilic but the surface structures induced an increase in θ_{diiodo} and $\theta_{hexadecane}$, this increase can be explained with the Cassie-Baxter equation even if here the droplets were in an intermediate state. Indeed, a pinning of the three-phase contact line due to the presence of specific surface topographies can induce this effect.[41-43]

TABLE 2 Contact angles for water, diiodomethane and hexadecane of the "smooth" polymer surfaces.

Polymer	θ^Y_{water}	θ^Y_{diiodo}	$\theta^Y_{hexadecane}$
PProDOT-F_4H_2	98.0	63.4	42.9
PProDOT-F_4H_4	101.3	70.2	42.7
PProDOT-F_4H_6	103.0	63.5	38.1

CONCLUSIONS

Here, has been shown the possibility to obtain superhydrophobic surfaces with good oleophobic properties replacing long fluorocarbon chains, due to their bioaccumulative potential, by shorter ones. The results demonstrate the possibility to achieve such properties by electropolymerization of novel 3,4-propylenedioxythiophene derivatives containing both a short fluorocarbon chain (perfluorobutyl) and a hydrocarbon chain of various length (ethyl, butyl and hexyl). The lowest adhesion properties (Lotus effect)[36] were surprisingly obtained with the shortest alkyl chains due to the presence of nanofibers microstructures on the surface while the longest alkyl chains led to nanosheets with higher adhesion (Petal effect).[40] These materials can be envisaged for various applications including biomedical applications.[4,5]

ACKNOWLEDGEMENTS

The group thanks Jean-Pierre Laugier of the CCMA (Univ. Nice Sophia Antipolis) for the realization of the SEM images. This project was supported by JSPS [KAKENHI, Grant-in-Aid for Young Scientists (A), No. 23685034], RCUK [through EPSRC EP/K020676/1] and ANR-13-G8ME-0003 under the G8 Research Councils

Initiative on Multilateral Research Funding - G8-2012.

REFERENCES AND NOTES

1. B. Bhushan, Y. C. Jung, K. Koch, *Philos. Trans. R. Soc., A* **2009**, *367*, 1631-1672.
2. Z. She, Q. Li, Z. Wang, L. Li, F. Chen, J. Zhou, *Chem. Eng. J.* **2013**, *228*, 415-424.
3. Y. Wang, J. Xue, Q. Wang, Q. Chen, J. Ding, *ACS Appl. Mater. Interfaces* **2013**, *5*, 3370-3381.
4. C.-H. Xue, J. Chen, W. Yin, S.-T. Jia, J.-Z. Ma, *Appl. Surf. Sci.* **2012**, *258*, 2468-2472.
5. Y. Lai, L. Lin, F. Pan, J. Huang, R. Song, Y. Huang, C. Lin, H. Fuchs, L. Chi, *Small* **2013**, *9*, 2945-2953.
6. a) H. S. Lim, S. G. Lee, D. H. Lee, D. Y. Lee, S. Lee, K. Cho, *Adv. Mater.* **2008**, *20*, 4438-4441; b) S. Taleb, T. Darmanin, F. Guittard, *RSC Adv.* **2014**, *4*, 3550-3555; c) T. Darmanin, F. Guittard, *ChemPhysChem* **2013**, *14*, 2947-2953.
7. a) T. Darmanin, J. Tarrade, E. Celia, F. Guittard, *J. Phys. Chem. C* **2014**, *118*, 2052-2057; b) Y. Shang, Y. Si, A. Raza, L. Yang, X. Mao, B. Ding, J Yu, *Nanoscale* **2012**, *4*, 7847-7854; c) T. Darmanin, F. Guittard, *J. Colloid Interface Sci.* **2013**, *408*, 101-106.
8. H. Bellanger, T. Darmanin, E. Taffin de Givenchy, F. Guittard, *Chem. Rev.* **2014**, *114*, 2694-2716.
9. T. Darmanin, F. Guittard, *Prog. Polym. Sci.* **2014**, *39*, 656-682.
10. T. Darmanin, E. Taffin de Givenchy, S. Amigoni, F. Guittard, *Adv. Mater.* **2013**, *25*, 1378-1394.
11. Y.-Z. Long, M.-M. Li, C. Gu, M. Wan, J.-L. Duvail, Z. Liu, Z. Fan, *Prog. Polym. Sci.* **2011**, *36*, 1415-1442.
12. C. Li, H. Bai, G. Shi, *Chem. Soc. Rev.* **2009**, *38*, 2397-2409.
13. C. Ding, Y. Zhu, M. Liu, L. Feng, M. Wan, L. Jiang, *Soft Matter* **2012**, *8*, 9064-9068.
14. H. Zhang, J. Wang, Z. Zhou, Z. Wang, F. Zhang, S. Wang, *Macromol. Rapid Commun.* **2008**, *29*, 68-73.
15. L. Xu, Z. Chen, W. Chen, A. Mulchandani, Y. Yan, *Macromol. Rapid Commun.* **2008**, *29*, 832-838.
16. T. Darmanin, F. Guittard, *J. Am. Chem. Soc.* **2009**, *131*, 7928-7933.
17. T. Darmanin, F. Guittard, *J. Am. Chem. Soc.* **2011**, *133*, 15627-15634.
18. O. Dunand, T. Darmanin, F. Guittard, *ChemPhysChem* **2013**, *14*, 2947-2953.
19. S.-C. Luo, S. S. Liour, H.-h. Yu, *Chem. Commun.* **2010**, *46*, 4731-4733.
20. H. Yan, K. Kurogi, H. Mayama, K. Tsujii, *Angew. Chem.* **2005**, *117*, 3519-3522; *Angew. Chem. Int. Ed. Engl.* **2005**, *44*, 3453-3456.
21. J. El-Maiss, T. Darmanin, E. Taffin de Givenchy, F. Guittard, *Macromol. Mater. Eng.*, DOI: 10.1002/mame.201300409.
22. M. Wolfs, T. Darmanin, F. Guittard, *Eur. Polym. J.* **2013**, *49*, 2267-2274.
23. T. Darmanin, F. Guittard, *Mater. Chem. Phys.*, DOI: 10.1016/j.matchemphys.2013.12.026.
24. S.-C. Luo, J. Sekine, B. Zhu, H. Zhao, A. Nakao, H.-h. Yu, ACS Nano 2012, 6, 3018-3026.
25. a) J. P. Giesy, K. Kannan, *Environ. Sci. Technol.* **2001**, *35*, 1339-1342; b) N. Kudo, Y. Kawashima, *J. Toxicol. Sci.* **2003**, *28*, 49-57.
26. a) M. Houde, J. W. Martin, R. J. Letcher, K. R. Solomon, D. C. G. Muir, *Environ. Sci. Technol.* **2006**, *40*, 3463-3473; b) J. M. Conder, R. A. Hoke, W. De Wolf, M. H. Russell, R. C. Buck, *Environ. Sci. Technol.* **2008**, *42*, 995-1003.
27. P. Lucas, M.A. Jouani, H. Trabelsi, A. Cambon, *J. Fluorine Chem.* **1998**, *92*, 17-22.
28. H. Trabelsi, S. Szoenyi, P. Reuter, E. Wehrli, S. Geribaldi, *Supramol. Chem.* **2001**, *13*, 583-591.
29. a) A. Drame, E. Taffin de Givenchy, S. Y. Dieng, S. Amigoni, M. Oumar, A. Diouf,

T. Darmanin, F. Guittard, *Langmuir* **2013**, *29*, 14815-14822; b) A. Drame, T. Darmanin, S. Y. Dieng, E. Taffin de Givenchy, F. Guittard, *RSC Adv.* **2014**, *4*, 10935-10943.
30. M. Wolfs, T. Darmanin, F. Guittard, *Polym. Rev.* **2013**, *53*, 460-505.
31. E. Poverenov, M. Li, A. Bitler, M. Bendikov, *Chem. Mater.* **2010**, *22*, 4019-4025.
32. R. N. Wenzel, *Ind. Eng. Chem.* **1936**, *28*, 988-994.
33. a) A. B. D. Cassie and S. Baxter, *Trans. Faraday Soc.* **1944**, *40*, 546-551; b) S. Baxter and A. B. D. Cassie, *J. Text. Inst., Trans.* **1945**, *36*, T67-T90.
34. T. Young, *Philos. Trans. R. Soc. London* **1805**, *95*, 65-87.
35. Y.Y. Yan, N. Gao, W. Barthlott, *Adv. Colloid Interface Sci.* **2011**, *169*, 80-105.
36. K. Koch, B. Bhushan, W. Barthlott, *Soft Matter* **2008**, *4*, 1943-1963.
37. Y. Zhang, Y. Chen, L. Shi, J. Li, Z. Guo, *J. Mater. Chem.* **2012**, *22*, 799-815.
38. Y. Yu, Z.-H. Zhao, Q.-S. Zheng, *Langmuir* **2007**, *23*, 8212-8216.
39. Y. Su, B. Ji, K. Zhang, H. Gao, Y. Huang, K. Hwang, *Langmuir* **2010**, *26*, 4984-4989.
40. L. Feng, Y. Zhang, J. Xi, Y. Zhu, N. Wang, F. Xia, L. Jiang, *Langmuir* **2008**, *24*, 4114-4119.
41. A. Marmur, *Soft Matter* **2013**, *9*, 7900-7904.
42. J. Bico, U. Thiele, D. Quere, *Colloids Surf., A* **2002**, *206* , 41-46.
43. K. Kurogi, H. Yan, K. Tsujii, *Colloids Surf., A* **2008**, *317*, 592-597.

GRAPHICAL ABSTRACT

Janwa El-Maiss, Thierry Darmanin, Elisabeth Taffin de Givenchy, Sonia Amigoni, Julian Eastoe, Masanobu Sagiska, and Frédéric Guittard

The aim of this work is to replace the use of long fluorocarbon chains due to their bioaccumulative potential in animals and humans. Superhydrophobic surfaces with high and low adhesion and with good oleophobicity are obtained by electropolymerization using a monomer containing both a hydrophobic chain and a short fluorocarbon chain.